City Research Online

City, University of London Institutional Repository

Citation: Diego-Ayala, U., Martinez-Gonzalez, P., McGlashan, N. & Pullen, K. R. (2008). The mechanical hybrid vehicle: an investigation of a flywheel-based vehicular regenerative energy capture system. Proceedings of the Institution of Mechanical Engineers, Part D: Journal of Automobile Engineering, 222(11), pp. 2087-2101. doi: 10.1243/09544070jauto677

This is the accepted version of the paper.

This version of the publication may differ from the final published version.

Permanent repository link: https://openaccess.city.ac.uk/id/eprint/4057/

Link to published version: https://doi.org/10.1243/09544070jauto677

Copyright: City Research Online aims to make research outputs of City, University of London available to a wider audience. Copyright and Moral Rights remain with the author(s) and/or copyright holders. URLs from City Research Online may be freely distributed and linked to.

Reuse: Copies of full items can be used for personal research or study, educational, or not-for-profit purposes without prior permission or charge. Provided that the authors, title and full bibliographic details are credited, a hyperlink and/or URL is given for the original metadata page and the content is not changed in any way.

City Research Online: http://openaccess.city.ac.uk/ publications@city.ac.uk

The Mechanical Hybrid Vehicle, an investigation of a flywheel-based vehicular regenerative energy capture system

U Diego-Ayala, P Martinez-Gonzalez, N R McGlashan, and **K R Pullen**
Department of Mechanical Engineering, Imperial College, London, SW7 2BX, UK

Abstract: Capturing braking energy by regeneration into an on board energy storage unit, offers the potential to reduce significantly the fuel consumption of vehicles. A common technique is to generate electricity in the motors of a hybrid electric vehicle when braking, and use this to charge an on board electrochemical battery. However, such batteries are costly, bulky and generally not amenable to fast charging as this affects battery life and capacity. In order to overcome these problems, a mechanical energy storage system capable of accepting and delivering surges of power is proposed and investigated. A scale physical model of the system, based around a flywheel, a planetary gear set and a brake, was built and operated in a laboratory. Tests showed that the proposed system could be used to store and provide braking energy between a flywheel and a vehicle, the latter emulated by an air-drag dynamometer. This validated the operating principle of the system and its computational model. Further, a computational analysis of a full size vehicle incorporating the mechanical energy storage system was conducted. The results showed that the utilisation of this system in a vehicle, when compared to a conventional vehicle, led to reductions in emissions and fuel consumption.

Keywords: regenerative braking, braking energy, hybrid vehicle, planetary gear set, epicyclic, flywheel.

NOTATION

A, B	= variables for PGS speed
CVT	= continuously variable transmission
GR_{C_CVT}	= gear ratio between main input shaft and CVT
GR_{C_fd}	= gear ratio between main input shaft and final drive
GR_{R_CVT}	= gear ratio between ring and CVT
I_{fw}	= inertia of the flywheel
PGS	= Planetary Gear Set
P_{fw_shaft}	= power in the flywheel's shaft
$R_{1,2}$	= number of teeth of ring gear for stage 1 and 2 respectively in double planetary gear set
$S_{1,2}$	= number of teeth of sun gear for stage 1 and 2 respectively in double planetary gear set
T_C	= torque in the carrier
T_{C_CVT}	= torque in the output of CVT
T_{Clutch_in}	= torque in the input of clutch
T_{Clutch_out}	= torque in the output of clutch
T_{CVT_in}	= torque in the input of CVT
T_{CVT_out}	= torque in the output of CVT
T_{fd}	= torque in the final drive's shaft
T_{fw}	= torque in the flywheel's shaft
T_{fwloss}	= torque loss at flywheel
T_R	= torque in the ring
T_{R_loss}	= torque loss at the ring
T_S	= torque in the sun
T_{S_loss}	= torque loss at the sun
T_{Shaft}	= torque in the main input shaft
VR_{Clutch}	= velocity ratio of clutch
VR_{CVT}	= velocity ratio of CVT
VR_{MAX}	= minimum velocity ratio of CVT
VR_{MIN}	= minimum velocity ratio of CVT
Δt	= time step for the simulation
$\Delta\omega_{fw}$	= change in flywheel angular speed for a given time step

η_{C_CVT} = efficiency at gear connection of CVT output and main input shaft

η_{C_fd} = efficiency at gear connection of main input shaft and final drive

η_{Clutch} = efficiency at clutch

η_{CVT} = efficiency at CVT

η_{PGS} = efficiency of the planetary gear set

η_{R_CVT} = efficiency at connection of ring and CVT

ω_C = angular speed of carrier

ω_{Clutch_in} = angular speed of input of clutch

ω_{Clutch_out} = angular speed of output of clutch

ω_{CVT_in} = angular speed of input of CVT

ω_{CVT_out} = angular speed of output of CVT

ω_{Dyna_exp} = experimental measurement of dynamometer's angular speed

ω_{fd} = angular speed of final drive

ω_{fw} = average flywheel angular speed

ω_{fw_exp} = experimental measurement of flywheel's angular speed

ω_R = angular speed of ring

ω_{Ring_exp} = experimental measurement of ring's angular speed

ω_S = angular speed of sun

1. INTRODUCTION

Hybrid Electric Vehicles (HEVs) are becoming familiar as vehicles able to operate with the comfort and performance typical of vehicles with conventional transmissions (henceforth denoted conventional vehicles). They offer two attractive features when operating in urban environments: significant reduction in fuel consumption coupled with low emissions. The powertrains in these vehicles typically consist of an internal combustion engine, to provide baseline drive power, and batteries with electric motors to provide acceleration assistance, low speed drive and braking energy recovery [1]. Their improved performance is due to a number of factors, but critically, the powertrain is able to operate in conjunction with a secondary power source (the battery and associated motor/generators). This secondary power source allows the engine to operate more efficiently and protects it from the worst transient power demands. The engine can also be turned off and seamlessly restarted. In addition, there is the capability to partially store regenerative energy [2-4].

Given the performance shown by HEVs, manufacturers present them as an alternative to conventional vehicles; however, their high cost relative to the savings in fuel consumption is undermining their commercial viability. The cost differential with conventional vehicles is to a degree given by the addition of a particular element in the powertrain: the batteries and associated power converter, which are the typical secondary energy storage means of HEV. Despite great efforts by researchers and manufacturers, the cost of state of the art batteries suitable for vehicular application is still high [5-7]. Apart from their cost, batteries also suffer technical drawbacks such as low power to weight ratio, low energy density, high demand for temperature control, and uncertainty of lifetime with vehicular usage [8, 9]. Given that HEVs require batteries, the question was raised whether it was possible to use some other type of secondary energy storage. The answer was the use of a high-speed flywheel. The use of flywheels in hybrid vehicles has been proposed by a number of authors [10-13], but typically this involves the use of a motor generator to transmit power to and from the flywheel. This type of system carries a substantial efficiency penalty, due to the mechanical-electrical-mechanical energy conversion required. A different approach is to use a mechanical transmission, giving rise to the concept of the Mechanical Hybrid Vehicle (see Figure 1). This approach is characterised by the ease with which it can be implemented in a conventional vehicular powertrain. Of the few studies found in the literature on flywheel-based mechanical transmissions, these require substantial modifications to the powertrain and are oriented to the use of the flywheel to enhance engine operation. For example, for the hybrid powertrain built by the Swiss Federal Institute of Technology [14], the flywheel is used to supplement engine power output during periods of high power demand but the capture of braking energy can only be maintained for a short time. Similarly, in the hybrid transmission developed at the University of Eindhoven [15-17] the flywheel is used to boost power and protect the engine from low part-load efficiency operation, with only limited regenerative braking being attempted.

This paper discusses the operating principle of a mechanical energy storage system capable of capturing a major portion of the available regenerative energy. It presents experimental validation of the system, and discusses two possible implementations of the system in a conventional vehicle. The performance of the resulting hybrid vehicles is then assessed with a computer model.

2. THE MECHANICAL ENERGY STORAGE SYSTEM

Given that the mechanical energy storage system was designed to avoid substantial modifications to a conventional powertrain, its design is kept as simple as possible and it is integrated in parallel with a conventional transmission and engine. The major components of the system are a mechanical coupled high-speed flywheel as an energy storage unit, and a planetary gear set (PGS) used as a power flow controller and transmission element.

Two powertrain version systems incorporating the mechanical energy storage system and the PGS, shown in Figure 1, will be discussed in this article:

- The Brake-only system, which uses a mechanical brake at the ring gear of the PGS to control power flow.
- The CVT-brake system, which adds a continuously variable transmission (CVT) to the Brake-only system between the PGS and input shaft, thus extending the range of operation of the energy storage system.

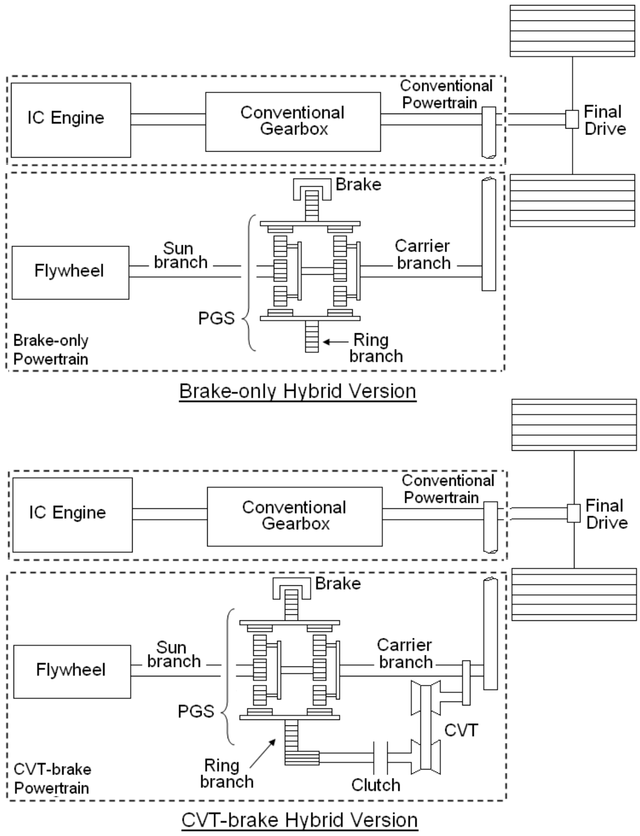

Figure 1. Schematic of Brake-only and CVT-brake versions of the mechanical hybrid vehicle.

The flywheel is based on an actual design developed by Shah [18]. This is a 0.11 kg·m^2 state of the art flywheel made of a multi-layered helical wound carbon fibre. The flywheel is operated under vacuum conditions maintained with the aid of non-contact, magnetic fluid ring seals. It was successfully tested spinning in vacuum at a speed up to 22,000 rpm.

The flywheel's angular velocity is independent of the vehicle's speed and it can vary from zero to tens of thousands of RPM. This requires high and continuous speed variations to mechanically couple the flywheel with the vehicle's final drive, which can be accomplished by two-stage PGS. The operation of this device will be explained in detail in section 2.1. The high speed of the flywheel is one the most important characteristics of this system; for example, in the powertrain proposed by the University of Eindhoven, the flywheel operates at low speed because it interacts directly with the engine; in contrast, the system proposed here operates directly in the final drive with a flywheel running at high speed independently of the prime propulsion unit used in the vehicle.

As shown in the figure above, the planet gears of the first-stage are coupled to the input shaft coming from the wheels (henceforth denoted as the carrier branch); the sun gear of the second-stage to the flywheel (henceforth denoted as the sun branch); and the ring gear, common to both stages, is connected to either a frictional brake, or a brake and CVT system. The elements connected to the ring branch will exert control of power flow through the system.

Both hybrid powertrains have the same modes of operation, which are:

1. Regenerative Braking (RB). In this mode, the flywheel captures kinetic energy from the vehicle as it decelerates.
2. Flywheel Assisted Acceleration (FA). In this mode, energy withdrawn from the flywheel is used to accelerate the vehicle.
3. Neutral (N). In this mode, the components of the system rotate freely without any transfer of energy between the flywheel and vehicle taking place.

Since the energy storage system is installed in parallel with the conventional powertrain, the hybrid vehicle retains the full capabilities of a conventional vehicle. To accomplish this mode of operation, the hybrid powertrain would simply operate in neutral mode.

2.1. Principle of Operation of the Planetary Gear Set

At the heart of the hybrid powertrain is the PGS, which controls energy flow between the flywheel and the vehicle. This type of transmission is commonly used where a high ratio of reduction is required in a compact space [19]. A PGS was selected instead of a single CVT as it provides superior ratio coverage and efficiency [20], while providing the continuous transmission ratios of CVTs.

This variability is achieved because planetary gear boxes are systems with two degrees of freedom. Such operation is related to the speed equilibrium of the branches for the PGS, whose governing equation is given by [21]:

$$\omega_C = A\omega_R + B\omega_S \tag{1}$$

where ω_C, ω_R , ω_S = speed of carrier, ring, and sun respectively, and A and B are constants of the PGS that describe the kinematics of the branches; the constants for A and B in equation (1) of the two-stage PGS are given by:

$$A = \frac{R_1(S_2 + R_2) + S_1R_2}{(S_1 + R_1)(S_2 + R_2)} \tag{2}$$

$$B = \frac{S_1S_2}{(S_1 + R_1)(S_2 + R_2)} \tag{3}$$

where S, R = number of teeth of the sun and ring gears respectively, and subscripts 1 and 2 refer to the first and second stages of the PGS.

Equation (1) implies that, for any given combination of sun (flywheel) and carrier (vehicle) speed, there is a critical equilibrium speed at which the ring will rotate . If the ring speed is forced to vary, energy transfer will occur and the speed of the sun and carrier will vary to comply with the equilibrium speed in the gearbox. This kinematic relationship can be pictured using a nomogram in which the carrier speed always lies on a line of value x = 0, the ring speed lies on a line of value x = -B and the sun speed lies on a line of value x = A. With this arrangement, for a given speed of any two branches, the speed of the third branch can be established by observation.

By way of example, Figure 2 illustrates the equilibrium speed for a PGS with A = 0.9 during regenerative braking. It can be seen that as the ring and carrier (vehicle) decelerate, the sun (flywheel) accelerates, maintaining the linear kinematic relationship as defined in equation (1). This relationship will be valid for both versions of the hybrid powertrain.

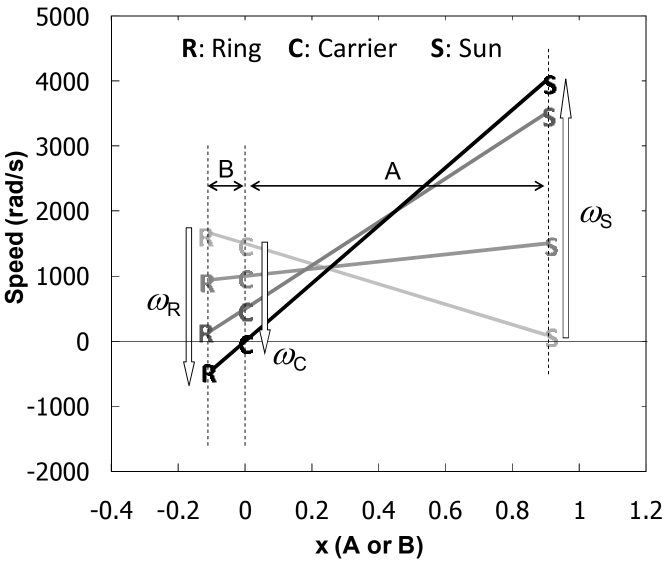

Figure 2. Visual example of equilibrium speeds in the PGS branches during regenerative braking.

The energy flow through the system can be explained by considering the torque equilibrium in the gearbox. Acting torques in a PGS can be calculated from the torque of one of its branches. Given a known torque in the carrier (T_C), the torque in the ring (T_R) and sun (T_S) are given by [21]:

$$T_R = -AT_C \tag{4}$$

$$T_S = -BT_C \tag{5}$$

Equations (4) and (5) indicate that for a given torque in the carrier, there is an opposite and proportional torque in the ring and the sun. The flow of energy between particular components is determined by the direction of torque and rotational speed at each branch. The convention used in this article is that having both speed and torque in the same direction indicates energy entering the PGS; conversely, opposite directions indicate energy leaving. It is therefore possible to control power flow in the system by applying a torque in the ring. This can be shown by examining in detail the modes of operation of the hybrid system:

During RB mode, as shown in Figure 3, all branches of the PGS rotate in the same direction. In this state, a torque opposite to the speed is applied at the ring so that it decelerates. Given the combination of torque and speed, energy flows from the carrier to the sun and ring, thus transmitting part of the kinetic energy of the vehicle to the flywheel. By inspection of Figure 2 it is evident that as the flywheel is charged with energy, the ring will reach a rest position before the vehicle (carrier) comes to a standstill. Thereafter no more regenerative braking can take place and conventional brakes are used for the final braking of the vehicle.

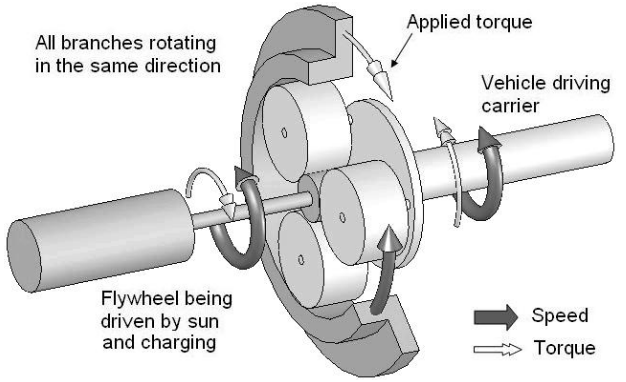

Figure 3. Regenerative Braking (RB) mode.

Once the flywheel has been charged with sufficient energy to accelerate the vehicle, it is ready to deliver power via the PGS and accelerate the vehicle (see Figure 4). With the vehicle initially at rest and the flywheel spinning at high speed, the critical speed of the ring will be in a negative direction (as in the darkest line in Figure 2). FA mode is initiated by again applying a torque in the ring to decelerate it. With the combination of torques and speeds (as shown in Figure 4), energy will transfer from the sun to the carrier causing the vehicle to accelerate with energy from the flywheel.

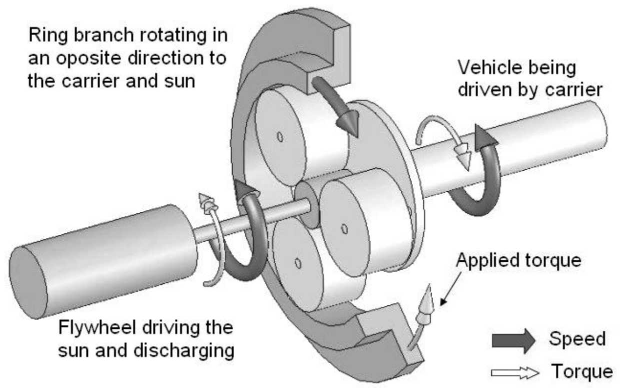

Figure 4. Flywheel Assisted Acceleration (FA) mode

During Neutral mode, no torque is applied at the ring and it therefore rotates at whatever equilibrium speed is required given the speed of the flywheel and vehicle. In this mode there is no transfer of energy between any of the branches.

Both systems studied use the same principle in controlling energy flow but the application of the control torque in the ring branch of the PGS is what differentiates them.

2.2. Equations of the Brake-only Powertrain Version

The brake-only system uses a friction brake at the ring of the PGS, as shown in Figure 1, to apply the necessary torque to control energy flow in the system. It is therefore only capable of decelerating the ring, which means that it must be rotating in a positive direction (as defined in Figure 2) when in Regenerative Braking mode and in a negative direction when in Flywheel Assisted Acceleration mode. This brake has no special requirements apart of being robust enough to dissipate the required energy.

The performance of the PGS follows the equations (1) to (5). However, the losses at the gearbox should also be included by accounting for its efficiency (η_{GB}). Torque losses at the sun (T_{S_loss}) and ring (T_{R_loss}) are calculated, depending on the direction of energy flow, with:

During Regenerative Braking (T_C>0)

$$T_{S\_loss} = -BT_C(\eta_{GB} - 1) \quad (6)$$

$$T_{R\_loss} = -AT_C(\eta_{GB} - 1) \quad (7)$$

During Flywheel Assisted Acceleration (T_C<0)

$$T_{S\_loss} = -BT_C(1/\eta_{GB} - 1) \quad (8)$$

$$T_{R\_loss} = -AT_C(1/\eta_{GB} - 1) \quad (9)$$

Given the inclusion of these torques, the equilibrium for the transmission should comply with

$$T_C + T_R + T_{R\_loss} + T_S + T_{S\_loss} = 0 \quad (10)$$

Therefore, the torque at the sun and ring should be calculated with the inclusion of the mechanical efficiency as presented below.

During Regenerative Braking (T_C>0)

$$T_S = -BT_C\eta_{GB} \quad (11)$$

$$T_R = -AT_C\eta_{GB} \quad (12)$$

During Flywheel Assisted Acceleration (T_C<0))

$$T_S = -BT_C/\eta_{GB} \quad (13)$$

$$T_R = -AT_C\eta_{GB} \quad (14)$$

The speed of the flywheel is based on the rotational equation of motion, which states that given a torque on the shaft of the flywheel (T_{fw_shaft}):

$$\Delta\omega_{fw} = \frac{(T_{fw\_shaft} - T_{fw\_loss})\Delta t}{I_{fw}} \quad (15)$$

where $\Delta\omega_{fw}$, I_{fw} and T_{fw_loss} are change in speed, inertia and torque losses of flywheel respectively.

For this equation T_{fw_shaft} equals T_S, but with the opposite sign to match torque equilibrium.

2.3. Equations of the CVT-brake Powertrain Version

The CVT-brake powertrain version consists of the same components as the brake-only version, but with the addition of a CVT. The addition of this mechanical component allows transmission of energy via the CVT branch after the ring has been stopped by the brake, thus extending the range of utilisation of the system and contributing to reduce ring brake losses. Therefore, when the CVT is not operating, equations of section 2.2 apply. During CVT operation, the equations shown in this section apply. Figure 5 shows the nomenclature used for describing the system. In this case the torque at the main input shaft (T_{Shaft}) is split into torque at the carrier (T_C) and torque at the CVT branch (T_{C_CVT}). The torque at the sun (T_S) and ring (T_R) are determined by the gear ratio of the PGS. The speed at the carrier (ω_C), ring (ω_R) and sun (ω_S) along with the torques determine power flow in the CVT and gearbox.

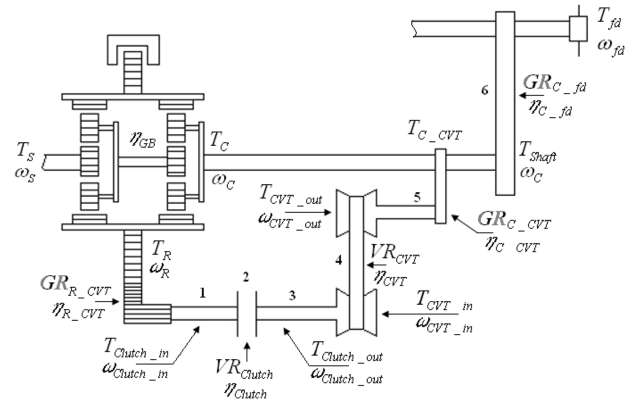

Figure 5. Nomenclature for the CVT-brake version of the mechanical Hybrid powertrain, showing Torque (*T*), speed (*ω*), gear ratio (GR), velocity ratio (VR) and efficiency (*η*) at the components are correlated with a subscript that depends on the mechanical component to which it refers. The numbers in the figure are correlated with the locations indicated in Table 1.

Ignoring powertrain losses, power equilibrium at the PGS is given by:

$$T_R\omega_R + T_C\omega_C + T_S\omega_S = 0 \tag{16}$$

While at the CVT power split it is given by:

$$T_{Shaft}\,\omega_C = T_C\omega_C + T_{C\_CVT}\,\omega_C \tag{17}$$

where,

$$T_R\omega_R = T_{C\_CVT}\,\omega_C \tag{18}$$

The overall power equilibrium between the input and the output of the mechanical hybrid powertrain is confirmed by combining equations (16), (17) and (18) and noting that:

$$T_{Shaft}\,\omega_C + T_S\omega_S = 0 \tag{19}$$

Therefore, the power transmitted through the CVT branch is found by solving equations (16) to (18) for a given initial speed at the flywheel.

These equations need to be modified to account for the existence of losses in the mechanical components of the system. Table 1 presents the full set of equations for the system (With reference to Figure 5).

Table 1. Equations for computational model of the CVT and PGS.

Location	**Speed equation**	**Torque equation (during Flywheel Assisted Acceleration)**[1]
1)Between ring and input of clutch	$\omega_{Clutch\_in} = -\omega_R * GR_{R\_CVT}$ (20)	$T_{Clutch\_in} = \dfrac{-T_R}{GR_{R\_CVT}}\eta_{R\_CVT}$ (21)
2)Clutch	$\omega_{Clutch\_out} = \omega_{Clutch\_in} * VR_{Clutch}$ (22)	$T_{Clutch\_out} = \dfrac{T_{Clutch\_in}}{VR_{Clutch}}\eta_{Clutch}$ (23)
3)Between output of clutch and input of CVT	$\omega_{CVT\_in} = \omega_{Clutch\_out}$ (24)	$T_{CVT\_in} = T_{Clutch\_out}$ (25)
4)CVT	$\omega_{CVT\_out} = \omega_{CVT\_in} * VR_{CVT}$ (26)	$T_{CVT\_out} = \dfrac{T_{CVT\_in}}{VR_{CVT}} * \eta_{CVT}$ (27)
5)Between output of CVT and main shaft	$\omega_{CVT\_out} = \omega_C * GR_{C\_CVT}$ (28)	$T_{C\_CVT} = T_{CVT\_out}GR_{C\_CVT}\eta_{C\_CVT}$ (29)
6)Between main shaft and final drive	$\omega_C = \omega_{fd} * GR_{C\_fd}$ (30)	$T_{Shaft} = \dfrac{T_{fd}}{GR_{C\_fd}} * \eta_{C\_fd}$ (31)

1 During Regenerative Braking the energy flow is reversed, thus the efficiency shown in the equations for torque is the inverse of the efficiency of the Flywheel Assisted Acceleration for each element.

With reference to the equations displayed in Table 1, incorporation of the losses at the CVT branch correlates the power through the CVT branch using:

$$T_{C\_CVT}\,\omega_C = T_R\,\omega_R\left(\eta_{R\_CVT}\,\eta_{Clutch}\,\eta_{CVT}\,\eta_{C\_CVT}\right) \quad (32)$$

which, combined with equation (17), gives for Flywheel Assisted Acceleration:

$$T_{Shaft}\,\omega_C = T_C\,\omega_C + T_R\,\omega_R\left(\eta_{R\_CVT}\,\eta_{Clutch}\,\eta_{CVT}\,\eta_{C\_CVT}\right) \quad (33)$$

equally for Regenerative Braking:

$$T_{Shaft}\,\omega_C = T_C\,\omega_C + \frac{T_R\,\omega_R}{\eta_{R\_CVT}\,\eta_{Clutch}\,\eta_{CVT}\,\eta_{C\_CVT}} \quad (34)$$

with the power equilibrium at the PGS during Flywheel Assisted Acceleration being given by:

$$T_R\,\omega_R + T_C\,\omega_C + T_S\,\omega_S\,\eta_{GB} = 0 \quad (35)$$

and during Regenerative Braking by:

$$T_R\omega_R + T_C\omega_C + \frac{T_S\omega_S}{\eta_{GB}} = 0 \quad (36)$$

Therefore, the solution of the variables at the system was achieved by solving, by means of successive iterations, equations (33) to (36) given a power demand or supply at the main shaft and an initial speed at the flywheel.

3. EXPERIMENTAL VALIDATION OF THE MECHANICAL ENERGY STORAGE SYSTEM

3.1. Physical Scale Test Bed

To validate the principle of operation of the proposed system, a test bed was developed to simulate the brake-only version described above. This configuration was chosen for the simplicity of its setup and ease of its control system, thus allowing for a simple system in which to test and study the kinematic behaviour of a flywheel-PGS system. The test bed and instrumentation used are shown in Figure 6.

The main components are:

- A high-speed flywheel made of mild steel with a diameter of 218 mm, and variable thickness ranging from 20 to 65 mm, giving an inertia of 0.11 kg·m^2. It operates at atmospheric pressure and, although it has significant aerodynamic losses, it is adequate to prove the operational principle of the energy storage unit.
- A dynamometer that emulates the energetic behaviour of a vehicle, allowing absorption and delivery of energy from and to the high-speed flywheel. It is made of a 20mm thick steel disc, with a diameter of 620 mm, giving a moment of inertia of 3.4 kg•m^2. The disc has blades installed around its periphery to emulate the aerodynamic losses of an actual vehicle. Its inertia and losses are scaled by a factor of approximately 40 to an actual mid-size vehicle.
- A double PGS transmission with kinematic values of A=0.9654, B=0.0346, as defined by equations (2) and (3), and a maximum torque capability of 25 Nm.
- A friction brake to decelerate the ring of the PGS and control energy flow.
- A 0.25 kW 2-Pole three-phase squirrel cage induction motor connected to the carrier to accelerate the dynamometer. This motor emulates the engine of the mechanical hybrid vehicle.

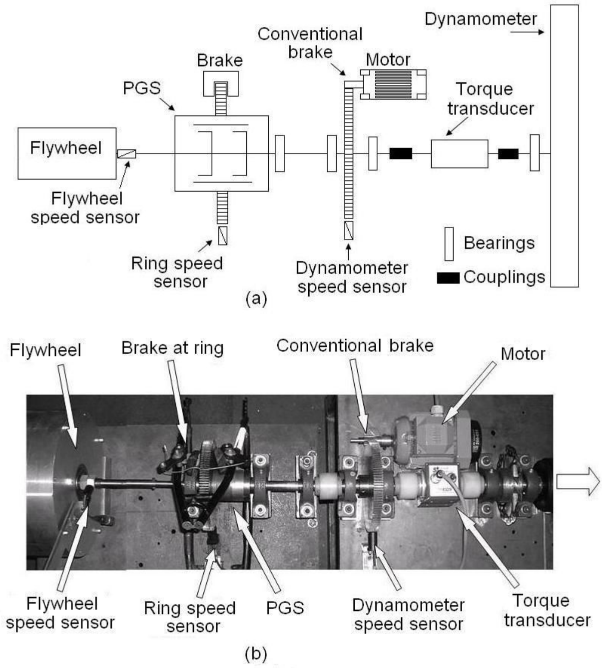

Figure 6. (a) Diagram and (b) photograph of the experimental test bed.

Rotational speed measurements were taken for all the branches of the PGS: ring, carrier (same as dynamometer) and sun (same as flywheel). Torque in the carrier branch was also measured.

These measurements were then analysed and compared to predictions of a computational model developed in-house to emulate the behaviour of the hybrid powertrain. This model uses the equations presented in section 2.

3.2. Experimental Results and Comparison with Computational Model

The purpose of the test bed was to validate the mathematic model by proving that kinetic energy from the dynamometer could be transferred to the flywheel, and vice versa by controlling the speed of the gearbox's ring. To do this, the dynamometer was subjected to a driving cycle consisting of three acceleration-deceleration periods. On each of those periods, the brake-only power train was used to store kinetic energy in the flywheel. Figure 7 (a) shows a test with the flywheel initiating from rest, whereas Figure 7 (b) shows the same cycle, but initiating with the flywheel already charged.

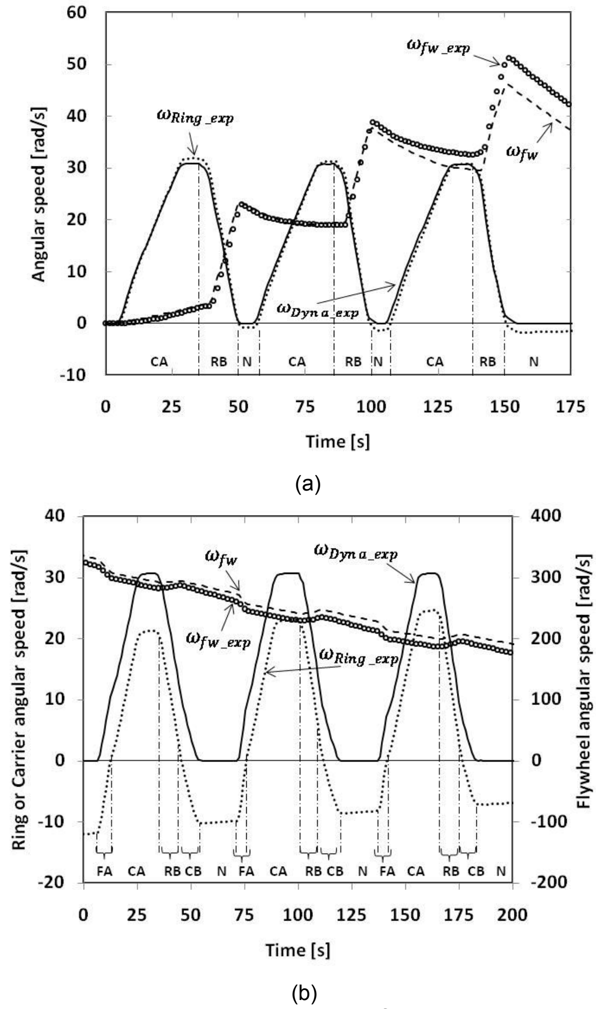

Figure 7. Experimental measurements of speed at dynamometer (ω_{Dyna_exp}), flywheel (ω_{fw_exp}) and ring (ω_{Ring_exp}) showing (a) only regenerative braking and (b) full hybrid vehicle operation. The dashed line corresponds to the speed at the flywheel predicted from the simulation (ω_{fw}). The segments on the bottom indicate the periods of flywheel assistance acceleration (FA), conventional acceleration (CA), regenerative braking (RB), and conventional braking (CB).

The aim of the first test (see Figure 7(a)) was to validate the regenerative braking principle, thus it was conducted with the flywheel starting from rest. The dynamometer was initially accelerated with the motor emulating conventional acceleration with an internal combustion engine (Period CA), and subsequently the brake at the ring was applied to provide regenerative braking (Period RB). Using this method, the flywheel was accelerated from a rest position to a speed of 45 rad/sec, validating the principle of the use of a PGS to transfer kinetic energy from the vehicle to the flywheel.

The test proved that regenerative braking using a flywheel and a PGS was possible by simply decelerating the ring branch of the PGS.

The second test (shown in Figure 7(b)) was designed to validate the hybrid vehicle's full operating cycle, which includes periods of flywheel assisted acceleration, conventional acceleration, regenerative braking and conventional braking. This test was initiated with the flywheel already charged, spinning at 343 rad/sec (3280 rpm), to ensure that sufficient energy was available to accelerate the dynamometer. Subsequently, transfer of energy between the flywheel and dynamometer was achieved by using all the available modes of the mechanical hybrid vehicle.

In order to validate the computational model, the torque and speed measurements of the dynamometer were loaded into the computer model and full simulations of the experiments were carried out. These simulation included estimates of transmission losses of the PGS, as well as windage and bearing losses of the flywheel.

The calculated and experimental angular speed of the flywheel (ω_{fw} and ω_{fw_exp} respectively) are shown in Figure 7, and serve the basis for the validation of the model. By inspecting Figure 7(a) it can be seen that the computational model of the system effectively simulates the transference of energy from the dynamometer to the flywheel every time the system was used in Regenerative Braking mode. Flywheel losses, clearly seen when the system operates in neutral, are also correctly predicted. By inspecting Figure 7(b), it can be seen that the same performance was seen in the second test. In this case, the acceleration and deceleration of the flywheel was properly simulated every time the energy storage system was in operation.

It was therefore concluded that a satisfactory numerical simulation was achieved from the simulation of the experimental tests, both at low and high flywheel speeds, thus validating the computational model.

4. SIMULATION OF A FULL SIZE MECHANICAL HYBRID VEHICLE

Computer simulations of a conventional vehicle and the two versions of the mechanical hybrid were performed for urban and extra-urban driving cycles, using a computational model of a Ford Focus Estate, developed by Diego-Ayala [22] and North [23]. In this model, steady-state engine maps with correction for engine warm up were used.

To assess the hybrid vehicle under city driving conditions, three widely accepted driving cycles were selected: the ECE, Artemis-urban and Hyzem-urban cycles[1], whose main data is shown in Table 2.

Table 2. Main parameters of driving cycles.

Description	ECE	Artemis -urban	Hyzem -urban
Distance travelled (km)	4.0	4.9	3.5
Duration (sec)	783	993	560
Maximum speed (km/h)	50	58.0	57.5
Average speed (with idling) (km/h)	18.3	17.7	22.4
Average accel. (m/sec^2)	1.1	2.9	2.2
Average decel. (m/sec^2)	-0.8	-3.2	-2.1
Idle time (sec)	256	283	139
Number of stops	12	22	5

4.1. The Conventional Vehicle Model

The vehicle utilised for the tests was a 1999 model year Ford Focus Estate with a 1.8L turbo diesel engine. Its main characteristics are summarised in Table 3.

Table 3. Specifications of the Ford Focus.

Description	Value
Gross vehicle weight (kg)	1441
Load weight (kg)	70
Frontal area (m^2)	2.06
Radius of wheels (cm)	28.2
Rolling friction coefficient (--)	0.009
Aerodynamic drag coefficient (--)	0.312

[1] The ECE cycle definition can be found in the EEC Directive 90/C81/01. The Artmeis-urban and Hyzem-urban cycle definition can be found in: André M. Real-world driving cycles for measuring cars pollutant emissions-Part A: The ARTEMIS European driving cycles. Bron, France: INRETS; June 2004. n°LTE 0411.

Gearbox transmission ratios (--)	3.25 / 1.99 / 1.14 / 0.77 / 0.60
Final drive ratio (--)	3.84
Maximum Engine speed (rpm)	4400
Maximum Engine power (kW)	65 @ 4400rpm
Maximum Engine torque (Nm)	184 @ 2000 rpm

4.2. The Hybrid Vehicle Models

4.2.1. The Brake-only Version Hybrid Vehicle Model

The Brake-only hybrid vehicle is obtained when the Brake-only system is integrated in parallel to a conventional powertrain. The main characteristics of the hybrid vehicle and its mechanical energy storage system are shown in Table 4. The value of the efficiency of the gearbox between carrier and final drive, used to solve equation (31), was set as a constant for simplicity.

Table 4. Main characteristics of mechanical energy storage system for the hybrid Ford Focus.

Description	Value
Additional weight due to hybrid system (kg)	100
Flywheel inertia (kg·m^2)	0.11
Efficiency at interconnection between carrier and final drive (--)	0.95
Value of constant *A* for PGS (--)	0.978
Value of constant *B* for PGS (--)	0.022
Gear ratio carrier/final drive (--)	0.5
Gear ratio carrier/CVT out (--)	2
Gear ratio ring/CVT in (--)	2

The efficiency map of the PGS and the flywheel losses are shown in Figure 8. The efficiency map of the PGS was developed based on existing maps from ADVISOR, whereas the flywheel's losses map, including bearing friction and windage losses, was developed based on experimental tests performed by Shah [18]. These values change dynamically as the simulation runs.

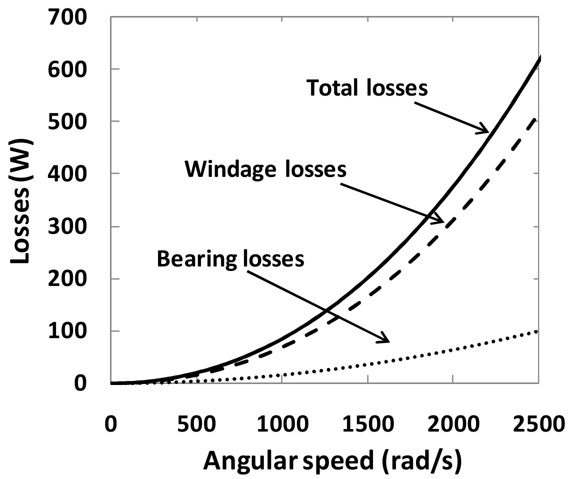

(a)

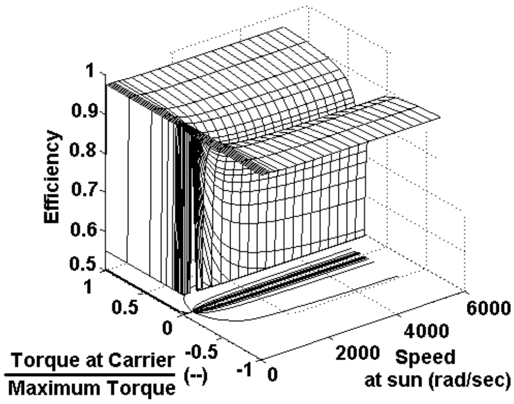

(b)

Figure 8. Maps of (a) losses at flywheel and (b) efficiency of PGS.

The hybrid vehicle will operate based on the speed of the sun (flywheel), ring and carrier (vehicle) and the torque demanded at the final drive.

The effect of the flywheel speed on the operation of the hybrid system depends on three pre-established values, namely:

- Flywheel maximum speed: The maximum safe operating speed of the flywheel.
- Flywheel minimum speed: The speed below which the flywheel will stop assisting an acceleration.
- Flywheel minimum operating speed: The minimum speed required before the flywheel initiates an acceleration assistance of the vehicle.

The magnitudes of these parameters are shown in

Table 5.

Table 5. Values for simulation of the hybrid Focus.

Description	Value
Flywheel minimum speed (rad/sec)	900
Flywheel minimum operating speed (rad/sec)	1200
Flywheel maximum speed (rad/sec)	2500

Depending on the speed of the flywheel and the operating state of the hybrid system, the engine will be turned on and off as required. If the engine is off and the vehicle is being accelerated with the flywheel, the engine would start with the starter motor. Since the FA acceleration of the vehicle will occur during a few seconds, the control system will have time to start the engine before it is required to take over from the flywheel's vehicle propulsion.

The control strategy implies that as long as the flywheel rotates below its minimum speed, the engine remains on and the energy storage system may only operate in neutral or in regenerative braking mode. The engine may only turn off once the flywheel has sufficient energy to adequately accelerate the vehicle (minimum operating speed) and the system is in a state where it may immediately operate in Flywheel Assisted Acceleration mode.

4.2.2. CVT-brake Version Hybrid Vehicle Model

The CVT model was designed in accordance with CVT's typically found in automotive applications. The speed ratio between output and input shaft of the model is between 0.4 and 2.5, which falls within the typical limit values[24-27]. The range of operation and efficiency of the CVT was emulated by means of an efficiency map (Figure 9) based on the results presented by Soltic [27]. This map shows an efficiency map for a dry belt variator, including hydraulic system. Since the efficiency is given by the instantaneous speed ratio and torque required, the value of η_{CVT} to solve equation (27) changes dynamically as the hybrid vehicle follows the drive cycle. The CVT will not be able to operate outside of a velocity ratio between 0.4 and 2.5, unless it is operating together with the clutch. Zero-load losses for the CVT were not included in the model.

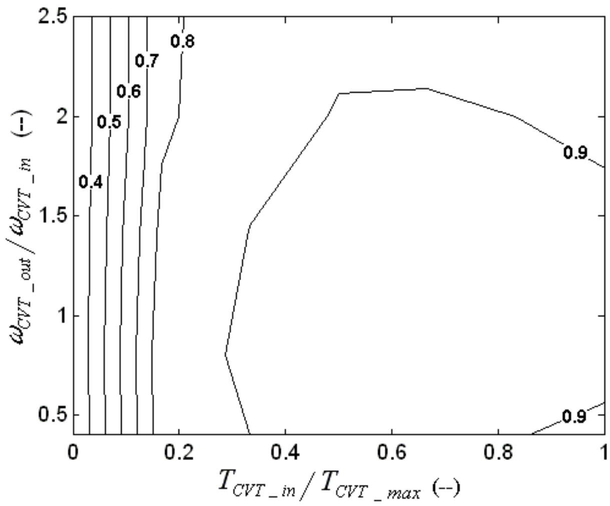

Figure 9. Variator efficiency map for CVT model correlating torque (Tin/Tmax) and velocity (Wout/Win).

The model of the clutch was designed to operate in similar fashion to a conventional clutch. When it is decoupled, both sides of the clutch are free to rotate in any direction and there is no transmission of energy. When it is slipping, one of the elements will apply torque to the other element in the same direction, eventually spinning it to the same speed. This operation does not require special characteristics, thus a wet-plate clutch would be sufficient to provide the desired effect in the transmission. The efficiency of the clutch is dependent on its speed ratio and it is taken to be 0.98 when fully coupled. An efficiency of 0.98 is also taken for the remaining mechanical components of equations (21) to (30).

4.3. Simulation Results and Discussion

The performance of the Bake-only and CVT-brake hybrids following the Urban-Hyzem cycle can be seen in Figure 10 (a) and (b).

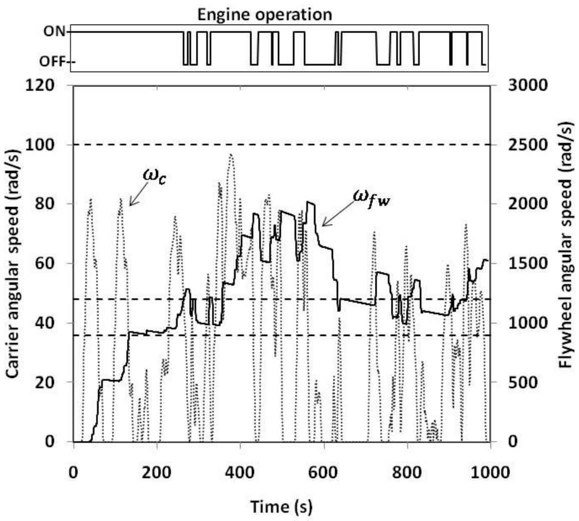

(a)

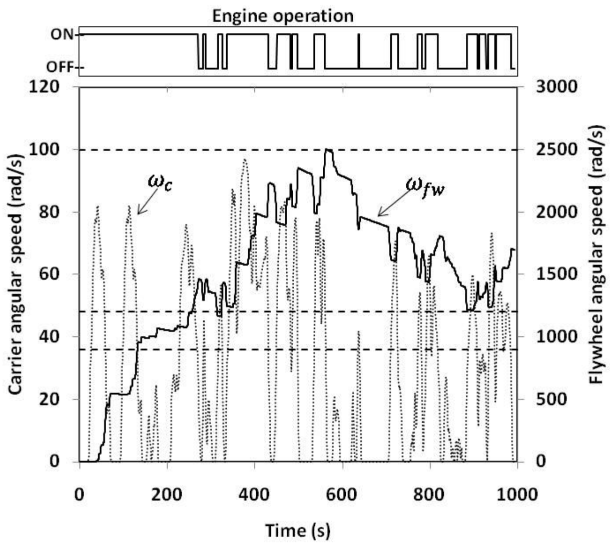

(b)

Figure 10. Performance of the (a) Brake-only hybrid and (b) CVT-brake hybrid vehicles following the Artemis-urban cycle, showing speeds of the flywheel (ωfw) and carrier (ωc). The continuous thin black line at the top, illustrates engine operation (Engine on or off); while the dashed thin black lines refer to flywheel maximum [upper], minimum operating and minimum [lower] speeds,

By inspecting the flywheel speed, it is evident that there is an intermittent transfer of energy between the carrier (i.e. vehicle) and flywheel as the vehicle is driven. The figures also show that the flywheel accelerates the vehicle shortly after it is charged with energy. This suggests that the performance of the system tends to maximise the re-utilisation of braking energy as the vehicle is driven.

Table 6 shows the fuel economy achieved by the conventional, Brake-only and CVT-brake vehicles over the three driving cycles used, as well as the vehicle's CO_2 emissions[2]. As expected, the lowest fuel economy is achieved by the conventional vehicle for all the driving cycles, with the CVT-brake hybrid enjoying higher gains in fuel economy than the Brake-only hybrid for all driving cycles.

Table 6 presents a breakdown of the energy losses for all the vehicle configurations and driving cycles. When a value is not reported it does not apply to that particular power train configuration.

Given the control strategy defined for the mechanical hybrid system, the engine intermittently turns on and off as the vehicle is being driven. This gives, as a result, a reduction in fuel consumption when compared to a conventional vehicle, despite an increase in vehicle weight. This improvement is due to both, the re-use of kinetic energy recovered when braking and the ability to switch off the engine.

Indeed the results suggest that the hybrid vehicle will achieve its highest potential in driving conditions requiring frequent stops (such as thus encountered in city driving conditions), as the hybrid vehicle will repeatedly regenerate the vehicle's kinetic energy during braking and use the flywheel to accelerate, thus providing more opportunities for the vehicle to to switch off the engine when the mechanical energy storage system is operating..

The greater fuel economy benefits were found in the Artemis-urban cycle which is the cycle with the highest number of stops and the most severe decelerations as shown in Table 2. The Brake-only hybrid exhibited an improvement of 11.3% in fuel economy on this cycle, which compares unfavourably with the CVT-brake system with a predicted saving of 25.7%. Since Regenerative Braking and Assisted Acceleration require the application of the brake at the ring for the Brake-only version, a considerable amount of energy is lost in the friction element. Furthermore, the mechanical energy storage system can only operate by braking the ring of the PGS so its operability is greatly reduced.

Table 6. Simulation results and breakdown of energy losses for the Conventional, Brake-only hybrid and CVT-brake hybrid vehicles.

	Description	ECE			Artemis-urban			Hyzem-urban		
		Conv.	Brake-only	CVT-brake	Conv.	Brake-only	CVT-brake	Conv.	Brake-only	CVT-brake
	Fuel economy (mpg UK)	31.6	33.0	35.0	28.0	31.1	35.1	30.5	33.1	34.0
	Change in fuel economy over conventional(mpg / mpg)	-	4.2%	10.7%	-	11.3%	25.7%	-	8.6%	11.8%
	Ultimate CO_2 emissions (gr/km)[2]	235	226	213	266	239	212	244	225	219
	Change in ultimate CO_2 emissions (gr/km / gr/km)	-	-4.0%	-9.7%	-	-10.1%	-20.4%	-	-7.9%	-10.5%
	% time the engine is OFF	0%	12.6%	22.4%	0%	23.9%	40.1%	0%	19.9%	23.8%
Energy distribution %	Energy content in Fuel (MJ)	12.86	12.34	11.62	17.95	16.12	14.28	11.74	10.80	10.50
	Engine losses during propulsion	71.1%	72.8%	73.9%	69.2%	70.8%	70.4%	71.3%	73.2%	72.4%
	Engine losses during idling	13.3%	10.5%	8.7%	9.6%	6.1%	4.3%	8.4%	5.0%	5.1%
	Gearbox transmission losses	3.9%	4.1%	4.4%	4.6%	4.9%	6.4%	4.8%	5.0%	5.7%
	Final drive transmission losses	0.9%	1.2%	1.6%	1.1%	1.8%	2.6%	1.0%	1.6%	2.0%
	Dissipated by conventional brakes	5.6%	1.1%	0.1%	10.8%	2.4%	0.5%	9.0%	1.5%	0.2%
	Rolling and aerodynamics losses	5.2%	5.7%	6.0%	4.7%	5.4%	6.1%	5.4%	6.1%	6.3%
	Dissipated in the ring of the PGS	-	3.0%	2.9%	-	6.2%	4.4%	-	5.2%	4.2%
	Transmission losses of PGS	-	0.5%	0.5%	-	0.9%	1.2%	-	0.8%	0.7%
	Aerodynamic and bearing losses in flywheel	-	0.4%	0.5%	-	0.7%	1.3%	-	0.5%	0.7%
	Remaining in flywheel at end of simulation	-	0.7%	1.0%	-	0.8%	1.1%	-	1.0%	2.1%
	Losses in CVT branch	-	-	0.3%	-	-	1.6%	-	-	0.5%

[2] Found in: EMEP/CORINAIR Emission Inventory Guidebook - 2006. 2006 21/12/2006:29.

As shown in Table 6, losses at the ring of the PGS are diminished in the CVT-brake version by using the CVT to provide the necessary torque at the ring of the PGS and using it at the same time as a transmission element. The CVT also increases the operability of the mechanical energy storage system as it can function by either decelerating or accelerating the ring of the PGS. The advantages of including the CVT in the system are clear as there is a consistent reduction in the heat released by the conventional brakes, and more importantly a consistent increase in the amount of time the energy storage system operates, greatly increasing the time the engine is switched off.

In addition, the operation of the energy storage system during initial acceleration is also of great importance as the flywheel is able to provide a higher power than the engine. This effect is also beneficial for the hybrid system, because having a high power available from the flywheel could justify a downsizing of the engine, which would even further increase the benefits of the hybrid system.

Therefore, the conclusion of this study is that the installation of the mechanical energy storage system in a conventional vehicle would potentially improve fuel economy and reduce emissions, but that its performance is greatly affected by the drive cycle in which the vehicle is driven. However, if the drive cycle profile is typical of a city driving, with, for example, a low average speed and continuous stops, it is likely that the overall efficiency of the hybrid vehicle would be enhanced and emissions be reduced. However, to avoid recirculation of power on the CVT-brake version hybrid, the operation of the CVT is restricted to the periods in which the ring of the PGS is negative, affecting the number of periods in which the system may operate. The optimisation of this system is recognised as a potential area of opportunity for further improvement of the mechanical hybrid powertrain.

5. CONCLUSIONS

The operating principle of the mechanical energy storage unit has been described and its operational principle tested in an experimental test bed. It has been demonstrated that the unit is able to capture, store and provide energy as demanded, proving the potential of this technology for hybrid vehicles.

A computational model of the system has been validated against the experimental results, and it has been shown that it is an appropriate tool for assessing the performance of the energy storage unit on a hybrid powertrain. The numerical simulations of the performance of a conventional vehicle and two different versions of a mechanical hybrid vehicle have been carried out with this model.

Fuel economy improvements of 11.3% for the Brake-only version and of 25.7% CVT-brake version were predicted for the Artemis-urban cycle. It was found that the implementation of such a hybrid system is better suited for vehicles that will operate in heavily congested traffic, since continuous stops/starts are advantageous for the recovery and re-utilisation of energy.

One particularly attractive feature is the ease by which a conventional powertrain can be adjusted to add hybrid capability. Unlike other forms of hybrids, this mechanical hybrid vehicle can be obtained by simply adding the mechanical energy storage system to a conventional powertrain, therefore the hybrid system can also be considered to be a “bolt-on” hybrid. No cost analysis has been carried out for the proposed design, however it is likely that the cost of its mechanical components will be substantially lower than the electrical components currently used in hybrid electric vehicles.

6. REFERENCES

[1] **C. C. Chan**. Electric vehicles charge forward. *Power and Energy Magazine, IEEE*, 2004, **2**(6), 24-33.

[2] **M. Duoba, H. Ng, and R. Larsen**. In-situ mapping and analysis of the Toyota Prius HEV engine. In Future Transportation Technology Conference and Exposition, Costa Mesa, California, August 21-23, 2000 (SAE paper 2000-01-3096).

[3] **L. B. Lave and H. L. MacLean**. An environmental-economic evaluation of

hybrid electric vehicles: Toyota's Prius vs. its conventional internal combustion engine Corolla. *Transportation Research Part D-Transport and Environment*, 2002, **7**(2), 155-162.

[4] **A. Taniguchi, N. Fujioka, M. Ikoma, and A. Ohta**. Development of nickel/metal-hydride batteries for EVs and HEVs. *J. Power Sources*, 2001, **100**(1-2), 117-124.

[5] **S. G. Chalk and J. F. Miller**. Key challenges and recent progress in batteries, fuel cells, and hydrogen storage for clean energy systems. *Journal of Power Sources*, 2006, **159**(1), 73--80.

[6] **E. Karden, S. Ploumen, B. Fricke, T. Miller, and K. Snyder**. Energy storage devices for future hybrid electric vehicles. *Journal of Power Sources*, 2007, **168**(1), 2--11.

[7] **T. Ozaki, H. B. Yang, T. Iwaki, S. Tanase, T. Sakai, H. Fukunaga, N. Matsumoto, Y. Katayama, T. Tanaka, T. Kishimoto, and M. Kuzuhara**. Development of Mg-containing MmNi5-based alloys for low-cost and high-power Ni-MH battery. *Journal of Alloys and Compounds*, 2006, **408-412**, 294--300.

[8] **P. Gifford, J. Adams, D. Corrigan, and S. Venkatesan**. Development of advanced nickel metal hydride batteries for electric and hybrid vehicles. *J. Power Sources*, 1999, **80**(1-2), 157-163.

[9] **H. Oman**. New energy management technology gives hybrid cars long battery life. In 34th Intersociety Energy Conversion Engineering Conference, Vancouver, Canada, 1999, 1999 (SAE paper 1999-01-2468).

[10] **T. A. Aanstoos, J. P. Kajs, W. G. Brinkman, H. P. Liu, A. Ouroua, R. J. Hayes, C. Hearn, J. Sarjeant, and H. Gill**. High voltage stator for a flywheel energy storage system. *IEEE Trans. Magn.*. 2001, **37**(1), 242-247.

[11] **B. Bolund, H. Bernhoff, and M. Leijon**. Flywheel energy and power storage systems. *Renewable and Sustainable Energy Reviews*, 2007, **11**(2), 235-258.

[12] **Y. Suzuki, A. Koyanagi, M. Kobayashi, and R. Shimada**. Novel applications of the flywheel energy storage system. *Energy*, 2005, **30**(11-12), 2128-2143.

[13] **J. Van Mierlo, P. Van den Bossche, and G. Maggetto**. Models of energy sources for EV and HEV: fuel cells, batteries, ultracapacitors, flywheels and engine-generators. *J. Power Sources*, 2004, **128**(1), 76-89.

[14] **P. Dietrich, M. K. Eberle, and H. U. Hörler**. Results of the ETH-Hybrid III-vehicle project and outlook. In International Congress and Exposition, Detroit, Michigan, March 1-4, 1999 (SAE paper 1999-01-0920).

[15] **S. W. Shen, A. Serrarens, M. Steinbuch, and F. Veldpaus**. Coordinated control of a mechanical hybrid driveline with a continuously variable transmission. *JSAE Review*, 2001, **22**(4), 453-461.

[16] **S. W. Shen, B. Vroemen, and F. Veldpaus**. IdleStop and Go: a way to improve fuel economy. *Vehicle System Dynamics*, 2006, **44**(6), 449--476.

[17] **B. Vroemen, A. Serrarens, and F. Veldpaus**. Hierarchical control of the Zero Inertia powertrain. *JSAE Review*, 2001, **22**(4), 519-526.

[18] **S. Shah**. The Design and Development of a High Speed Composite Flywheel for Hybrid Vehicles. PhD thesis in *Department of Mechanical Engineering*. London: Imperial College, 2006.

[19] **D. A. Hofmann**. Gearing for high speed motors. In IEE Colloquium on High Speed Bearings for Electrical Machines, 1997.

[20] **G. Mantriota**. Theoretical and experimental study of a power split continuously variable transmission system Part 1. *Proceedings of the Institution of Mechanical Engineers, Part D: Journal of Automobile Engineering*, 2001, **215**(7), 837-850.

[21] **M. Santoro**. A Hybrid-Propulsion Powertrain with Planetary Gear Set for a WD Vehicle: Analysis of Power Flows and Energy Efficiency. Report of Dresden University of Technology, 1998.

[22] **U. Diego-Ayala**. An investigation into hybrid power trains for vehicles with regenerative braking. PhD thesis in *Department of Mechanical Engineering*. London: Imperial College, 2007.

[23] **R. J. North, W. Y. Ochieng, M. A. Quddus, R. B. Noland, and J. W. Polak**. Development and Testing of a Vehicle Performance and Emissions Monitoring System. *Transport: Proceedings of the Institution of Civil Engineers*, 2005, **158**(3), 167-177.

[24] **T. Klaassen, B. Vroemen, B. Bonsen, K. van de Meerakker, M. Steinbuch, and P. A. Veenhuizen**. Modeling and simulation of an electro-mechanically actuated pushbelt type continuously variable transmission. In 3rd IFAC Symposium on Mechatronic Systems, 2004.

[25] **H. Lee and H. Kim**. Improvement in fuel economy for a parallel hybrid electric vehicle by continuously variable transmission ratio control. *Proc. Inst. Mech. Eng., Part D J. Automob. Eng.*, 2005, **219**(D1), 43-51.

[26] **C. Osornio Correa**. Characterisation of a flexible transmission for a hybrid electrical vehicle optimising power train performance [in Spanish]. PhD thesis in *Department of Mechanical Engineering*: Autonomous National University of Mexico (UNAM), 2006.

[27] **P. Soltic and L. Guzzella**. Performance simulations of engine-gearbox combinations for lightweight passenger cars. *Proc. Inst. Mech. Eng., Part D J. Automob. Eng.*, 2001, **215**(2), 259-271.